

Dear editor,

We appreciate the very positive second report from referee #2 expressing content with our reactions to the issues in his first report.

Then the referee raises further issues. Our responses to these are in *italic* and section numbers and line numbers refer to the marked-up version of the revised manuscript.

Referee #1:

I went through the authors response to my earlier comments and generally agree with the modifications they have made. The paper is more complete and better suited for publication.

My only other query is whether the authors noted any systematic changes in the relative errors for the two durations for the 12.5km runs compared to the 50km runs? This is an issue that comes up with RCM simulations often as the computational expense in the higher resolution runs is considerable. Any comments could be useful to others.

We analyse solely 12.5 km runs (EUR-11, line 203-204). Therefore, we are not able to give any qualified take on this query.

Other than this, I noted down some specific issues in the order I read the paper. these are:

l65 - Authors should note the following two papers which are relevant here

Kim, Y., et al. (2020). "Impact of bias correction of regional climate model boundary conditions on the simulation of precipitation extremes." *Climate Dynamics* 55(11): 3507-3526.

Kim, S., et al. (2020). "Quantification of Uncertainty in Projections of Extreme Daily Precipitation." *Earth and Space Science* 7(8).

The first paper assesses the impact on extreme precipitation simulations once lateral and lower boundary biases are corrected. This is directly relevant to the present study. The second presents estimates of uncertainty in extreme precipitation simulations after bias correction for a range of models. I suggest the second one as it may give some guidance to authors to contrast their uncertainty estimates against those presented in the paper to gauge the extent of improvements made.

The first paper is a work where the forcing boundary conditions are bias-corrected. This is a different approach from ours.

The second paper is it is about partition of variance between scenario, model and internal variability in GCMs. The paper by (Aalbers et al., 2018) is a more comprehensive study of the issue. We have added a sentence in the revised manuscript. (line 461)

l72 and 73 - the referenced studies are not directly relevant to the present work because of the psuedoCC run. A bias corrected run would be a more appropriate comparison as noted in the above two papers.

We are not able to identify the references of concern, since no references are given in these line numbers, neither in the raw nor in the annotated manuscript. Therefore, we are unable to react to this comment.

197 - I have long felt that in hydrological modelling settings, the issue of persistence is more important than simply correcting means. The Nesting Bias Correction papers and its variants in multivariate settings are my recommended alternatives where a water balance simulation is needed. I urge the authors to expand their discussion about bias correction to mention this line of thought. The paper below gives details of the software and how it should be used.

Mehrotra, R., et al. (2018). "A software toolkit for correcting systematic biases in climate model simulations." *Environmental Modelling and Software* 104: 130-152.

We have added a short line and the reference (line 680)

1205 - In my experience the fitting of the GPD creates instability in the shape and scale parameters, especially given the short record that are typically used. It would be good for the authors to discuss whether unstable parameter values resulted and whether the RE estimates are sensitive to such instability in a systematic manner.

We are a bit in doubt about referee #2 really means l. 205. It is not specified whether it is referring to the marked-up version or not. In any case, extreme value analysis has not been mentioned at that point. We have added a sentence about uncertainties of parameters in EVA (lines 300-303)

1328 - The 24h results show 3 cases where there is a decrease into the future. No such decrease is present in the hourly simulations. Is this a pattern that was common across the other regions the study focused on? Would there be any reason for this? Perhaps linked to the instability in the GPD parameters?

Line 328 is before any mentioning of results. Could the referee mean l. 428? A similar behaviour is seen in other regions. We have added a sentence about this (line 460-461)

Editor:

In addition, a minor suggestion from my side - consider changing the label in the y-axis in Figure 4 to "Precipitation intensity [mm]"

We think the term 'precipitation intensity' means a rate (mm /h). We will change the label to 'precipitation sum', which we use in this work (see line. Xx)

Other changes:

Text have been adjusted for better readability.

Reference list format has been changed to conform to journal standard

References:

Aalbers, E. E., Lenderink, G., van Meijgaard, E. and van den Hurk, B. J. J. M.: Local-scale changes in mean and heavy precipitation in Western Europe, climate change or internal variability?, *Clim. Dyn.*, 50(11–12), 4745–4766, doi:10.1007/s00382-017-3901-9, 2018.

Identifying robust bias adjustment methods for European extreme precipitation in a multi-model pseudo-reality setting

Torben Schmith¹, Peter Thejll¹, Peter Berg², Fredrik Boberg¹, Ole Bøssing Christensen¹, Bo Christiansen¹, Jens Hesselbjerg Christensen^{1,3,4}, Marianne Sloth Madsen¹, Christian Steger⁵

¹ Danish Meteorological Institute, ~~Lyngbyvej 100, 2100~~ Copenhagen-Ø, Denmark

² Swedish Meteorological and Hydrological Institute, Hydrology Research Unit, Norrköping, Sweden

³ Physics of Ice, Climate and Earth, Niels Bohr Institute, University of Copenhagen, ~~2100~~ Copenhagen-Ø, Denmark

⁴ NORCE Norwegian Research Centre, Bjerknes Centre for Climate Research, ~~5007~~ Bergen, Norway

⁵ Deutscher Wetterdienst, ~~Frankfurter Straße 135, 63067~~ Offenbach, Germany

Correspondence: Torben Schmith (ts@dmi.dk)

Abstract

Severe precipitation events occur rarely and are often localized in space and of short duration; but they are important for societal managing of infrastructure. Therefore, there is a demand for estimating future changes in the statistics of occurrence of these rare events. These are often projected using data from Regional Climate Model (RCM) simulations combined with extreme value analysis to obtain selected return levels of precipitation intensity. However, due to imperfections in the formulation of the physical parameterizations in the RCMs, the simulated present-day climate usually has biases relative to observations; these biases can be in the mean and/or in the higher moments. Therefore, the RCM results are adjusted to account for these deficiencies. However, this does not guarantee that adjusted projected results will match future reality better, since the bias may not be stationary in a changing climate. In the present work we evaluate different adjustment techniques in a changing climate. This is done in an inter-model cross-validation setup, in which each model simulation in turn plays the role of pseudo-observations, against which the remaining model simulations are adjusted and validated. The study uses hourly data from historical and RCP8.5 scenario runs from 19 model simulations from the EURO-CORDEX ensemble at 0.11° resolution. ~~Fields of return levels for selected return periods are calculated from which fields of selected return levels are calculated~~ for hourly and daily time scales based on 25 years long time slices representing present-day (1981-2005) and end-21st-century (2075-2099). The adjustment techniques applied to the return levels are based on extreme value analysis and include climate factor and quantile ~~-~~mapping approaches. Generally, we find that future return levels can be improved by adjustment, compared to obtaining them from raw scenario model data. The performance of the different methods depends on the time scale considered. On hourly time scale, the climate factor approach performs better than the quantile ~~-~~mapping approaches. On daily time scale, the superior approach is to simply deduce future return levels from pseudo-observations and the second best choice is using the quantile ~~-~~mapping approaches. These results are found in all European sub-regions considered. Applying the inter-model cross-validation against model ensemble medians instead of individual models does not change overall conclusions much.

43 **1 Introduction**

44 Severe precipitation events occur typically either as stratiform precipitation of moderate intensity or as
45 intense localized cloudbursts lasting up to a few hours only. Such extreme events may cause flooding with
46 the risk of loss of life and damage to infrastructure. It is expected that future changes in the radiative
47 forcing from greenhouse gases and other forcing agents will influence the large scale atmospheric
48 conditions, such as air mass humidity, vertical stability, the formation of convective systems, and typical
49 low pressure tracks. Therefore also the statistics of the occurrence of severe precipitation events will most
50 likely change.

51
52 Global climate models (GCMs) are the main tool for estimating future climate conditions. A GCM is a global
53 representation of the atmosphere, the ocean and the land surface, and the interaction between these
54 components. The GCM is then forced with observed greenhouse gas concentrations, atmospheric
55 compositions, land use, etc. to represent the past and present climate, and with stipulated scenarios of
56 future concentrations of radiative forcing agents to represent the future climate.

57
58 Present state-of-the art GCMs from the Coupled Model Intercomparison Project Phase 5 ([CMIP5, Taylor et](#)
59 [al., 2012](#)) and the recent Coupled Model Intercomparison Project Phase 6 ([CMIP6, Eyring et al., 2016](#))
60 typically have a grid spacing of around 100 km or even more. This resolution is too coarse to describe the
61 effect of regional and local features, such as mountains, coast lines and lakes and to adequately describe
62 convective precipitation systems ([Eggert et al., 2015](#)). To model the processes on smaller spatial scales,
63 dynamical downscaling is applied. Here, the atmospheric and surface fields from a GCM simulation are used
64 as boundary conditions for a regional climate model (RCM) over a smaller region with a much finer grid
65 spacing, at present typically around 10 km or even less.

66
67 An alternative to dynamical downscaling is statistical downscaling. Here large-scale circulation patterns
68 (e.g. the North Atlantic Oscillation) are related to small-scale variables, such as precipitation mean at a
69 station. One assumes that the large-scale circulation pattern is modelled well by the GCM and therefore
70 the approach is called perfect prognosis. Using the relationship with the small-scale variables, calibrated on
71 observations, one can obtain modelled local-scale variables (present-day and future) from the modelled
72 large-scale patterns. A recent overview of these methods and validation of them can be found in Gutiérrez
73 et al. ([2019](#)).

74
75 The ability of present-day RCMs to reproduce observed extreme precipitation statistics on daily and sub-
76 daily time scales is essential and has been of concern. Earlier studies analysing this topic have mostly
77 focused on a particular country, probably due to the lack of sub-daily observational data covering larger
78 regions, such as e.g. Europe. Thus, Hanel and Buishand ([2010](#)), Kendon et al. ([2014](#)), Olsson et al. ([2015](#))
79 and Sunyer et al. ([2017](#)) studied daily and hourly extreme precipitation in different European countries and
80 reached similar conclusions: first that the bias of extreme statistics decreases with smaller grid spacing of
81 the model, and second that extreme statistics for 24 h duration are satisfactorily simulated with a grid
82 spacing of 10 km, while 1 h extreme statistics exhibits substantial biases even at this resolution. Recently,
83 Berg et al. ([2019](#)) evaluated high resolution RCMs from the EURO-CORDEX ensemble ([Jacob et al., 2014](#))
84 [also used here](#) and reached similar conclusions for several countries across Europe: RCMs underestimate
85 hourly extremes and give an erroneous spatial distribution.

86

87 Extreme convective precipitation of short duration is thus one of the more challenging phenomena to
88 represent physically accurate in RCMs. The reason is that convective events take place on a spatial scale
89 comparable to the RCM grid spacing of presently around 10 km. Therefore, the convective plumes cannot
90 be directly modelled. Instead, the effects of convection are parametrised, i.e. modelled as processes on
91 larger spatial scales ([Arakawa, 2004](#)). Thus, the inability to reproduce these short duration extremes can be
92 explained by the imperfect parametrization of sub-grid scale convection ([Prein et al., 2015](#)), which generally
93 leads to too early onset of convective rainfall in the diurnal cycle and subsequent dampening of the build-
94 up of convective available potential energy ([Trenberth et al., 2003](#)).

95

96 Thus, even RCMs with their small grid spacing may exhibit systematic biases for variables related to
97 convective precipitation. If there is a substantial bias, we should consider *adjusting* for this in a statistical
98 sense before any further data analysis. Such adjustment techniques are thoroughly discussed, including
99 requirements and limitations, in Maraun ([2016](#)) and Maraun et al. ([2017](#)). There are basically two main
100 adjustment approaches. In the *delta-change* approach, a transformation is established from the present to
101 the future climate in the model run. This transformation is then applied to the observations to get the
102 projected future climate. In the *bias correction* approach, a transformation is established from present
103 model climate data to the observed climate and this transformation is then applied to the future model
104 climate to obtain the projected future climate.

105

106 Both adjustment approaches come in several flavours. In the simplest one, the transformation consists of
107 an adjustment of the mean, in the case of precipitation by multiplying the mean by a factor. In the more
108 elaborate flavour, the transformation is defined by quantile_-mapping, preserving also the higher moments.
109 Quantile_-mapping can use either empirical quantiles or analytical distribution functions. The ability of
110 quantile_-mapping to reduce bias has been demonstrated for daily precipitation in present-day climate
111 using observations, which are split into calibration and validation samples ([Piani et al., 2010; Themeßl et al.,](#)
112 [2011](#)).

113

114 Bias adjustment techniques originate in the field of weather and ocean forecast modelling, where they are
115 known as model output statistics (MOS). Here output from a forecast model is adjusted for model
116 deficiencies and local features not explicitly resolved by the model. Applying similar adjustment techniques
117 to climate model simulations, however, has a complication not present in forecast applications: Climate
118 models are set up and tuned to present-day conditions and verified against observations, but then applied
119 to future changed conditions without any possibility to directly verify the model's performance under these
120 conditions. Therefore, showing that bias adjustment works for present-day climate is a necessary but not
121 sufficient condition for the adjustment to work in the changed climate.

122

123 A central concept of adjustment methods is the assumption of *stationarity* of the bias. For bias correction
124 this means that the transformation from model to observations is unchanged from the present-day climate
125 to the future climate, while for delta-change the transformation from present-day climate to future climate
126 is unchanged from model to observations. In the ideal case of stationarity being fulfilled, the adjustment
127 methods will work perfectly and produce perfect future projections. If stationarity is not fulfilled,
128 adjustment may improve projections, or in the worst cases they may degrade projections, compared to

129 using raw model output. We also note that the adjustment methods themselves may influence the climate
130 change signal of the model, depending on the bias and the method used (Berg et al., 2012; Haerter et al.,
131 2011; Themeßl et al., 2012)(Haerter et al. 2011; Berg et al. 2012; Themeßl et al. 2012).
132

133 Stationarity has been debated in recent years in the literature (e.g. Boberg and Christensen, 2012; Buser et
134 al., 2010). Kerkhoff et al. (2014) review and discuss two hypotheses: 1) constant bias: unchanged between
135 present-day and future (i.e. stationarity) and 2) constant relation: bias varies linearly with the signal. Van
136 Schaeybroeck and Vannitsem (2016) used a pseudo-reality setting with a simplified model and found large
137 changes in the bias between present-day and future for many variables and violation of both constant bias
138 and constant relation hypothesis. Chen et al. (2015) concluded that precipitation bias is clearly non-
139 stationary over North America in that variations in bias is comparable to the climate change signal.
140 Velázquez et al. (2015) used a pseudo-reality setting involving two models and concluded that constancy of
141 bias was violated for both precipitation and temperature on monthly time scale. Hui et al. (2019) used a
142 pseudo-reality setting with GCMs and found significant non-stationarity of bias for annual and seasonal
143 temperatures. Besides, they point to a large effect on non-stationarity from internal variability.
144

145 ~~We also note that the adjustment methods themselves may influence the climate change signal of the~~
146 ~~model, depending on the bias and the method used (Haerter et al. 2011; Berg et al. 2012; Themeßl et al.~~
147 ~~2012).~~
148

149 To thoroughly validate adjustment methods, both a calibration dataset and an independent dataset for
150 validation are needed. There are two different approaches to obtain this. In split-sample testing, the
151 observations are divided into calibration and validation parts, often in the form of a cross-validation (e.g.
152 Gudmundsson et al., 2012; Li et al., 2017a, 2017b; Refsgaard et al., 2014; Themeßl et al., 2011). A variant is
153 differential split-sample testing (Klemeš, 1986), where the split in calibration/and validation parts is based
154 on climatological factors, such as wet and dry years, encompassing climate changes and variations into the
155 validation.
156

157 An alternative approach, which we use here, is *inter-model cross-validation*, as pursued by Maraun (2012),
158 Räisänen and Rätty (2013) and Rätty et al. (2014) and others. The rationale is here that the members in a
159 multi-model ensemble of simulations represent different descriptions of physics of the climate system, with
160 each of them being not too far from the real climate system. Thus, one member of the ensemble
161 alternatively plays the role of *pseudo-observations*, against which the remaining adjusted models are
162 validated. Thus, the trick is that we know both present and future pseudo-observations.
163

164 The advantage of inter-model cross-validation, is that the adjustment methods are calibrated under
165 present-day conditions and validated under future climatic conditions. Therefore, it embraces modelled
166 physical changes between present and future climate, as for instance a shift in the ratio between stratiform
167 and convective precipitation. In this respect it is a more realistic setting than validation based on split-
168 sample test. Also, model and pseudo-observations have the same spatial scale, thus avoiding comparing
169 pointwise observations with area-averaged model data, as is done in the split-sample testing. On the other
170 hand, the method assumes that the modelled present-day is not too different from observations. If this is

171 violated, the method will give too optimistic error estimates compared to what can be expected in the real
172 World. Please cf. also further discussion in Section 5.2.

173

174 Inter-model cross-validation has been applied on daily precipitation to evaluate different adjustment
175 methods (Räty et al., 2014). Here we apply a similar methodology European-wide to extreme precipitation
176 on hourly and daily time scales. This has been made possible with the advent of the EURO-CORDEX, a large
177 ensemble of high-resolution RCM simulations with precipitation at hourly time-resolution. Being more
178 specific, we apply the standard extreme value analysis to the ensemble of model data for present-day and
179 end-21st-century conditions to estimate return levels for daily and hourly duration. Then we will apply inter-
180 model cross validation on these return levels in order to address the following questions:

- 181 1. Do adjusted return levels perform better, according to the inter-model cross-validation, than using
182 raw model data from scenario simulations?
- 183 2. Is there any difference in performance between different adjustment methods?
- 184 3. Are there systematic differences in point 1 and 2, depending on the daily and hourly duration?
- 185 4. Are there regional differences across Europe in the performance of the different adjustment
186 methods?

187 Giving qualified answers to these questions can serve as important guidelines for analysis procedures for
188 obtaining future extreme precipitation characteristics.

189

190 The rest of the paper contains a description of the EURO-CORDEX data (Section 2) and a description of
191 methods used (Section 3). Then follow the results (Section 4), a discussion of these (Section 5) and finally
192 conclusions (Section 6).

193

194 2 The EURO-CORDEX data

195 The model simulations used here have been performed within the framework of EURO-CORDEX (Jacob et
196 al. (2014) ; <http://euro-cordex.net>), which is an international effort aimed at providing RCM climate
197 simulations for a specific European region (see Figure 1) in two standard resolutions with a grid spacing of
198 0.44° (EUR-44, ~50 km) and 0.11° (EUR-11, ~12.5 km), respectively. All GCM simulations driving the RCMs
199 follow the CMIP5 protocol (Taylor et al., 2012) and are forced with historical forcing for the period-years
200 1951-1850-2005 followed by the RCP8.5 scenario for the period-years 2006-2100 (until 2099 only for
201 HadGEM-ES).

202

203 We analyse precipitation data in hourly time-resolution from 19 different GCM-RCM combinations from the
204 EUR-11 simulations shown in Table 1 and we analyse two 25 year long time slices from each of these
205 simulations: a present-day time slice (years 1981-2005) and an end-21st-century time slice (years 2075-
206 2099).

207

208 All GCM-RCM combinations we use are represented by one realization only, and therefore the data
209 material used represents 19 different possible realisations of climate model physics, though acknowledging
210 that some GCMs/RCMs might originate from the same or similar model code and therefore may not be fully
211 independent. The EURO-CORDEX ensemble includes a few simulations, which do not use the standard EUR-

212 11 grid. These were not included in the analysis, since they should have been re-gridded to the EUR-11 grid
 213 which would dampen extreme events, thus introducing an unnecessary error source.

214

215 Table 1. Overview of the 19 EURO-CORDEX GCM-RCM combinations used. The rows show the GCMs while the columns
 216 show the RCMs. The full names of the RCMs are SMHI-RCA4, CLMcom-CCLM4-8-17, KNMI-RACMO22E, DMI-HIRHAM5,
 217 MPI-CSC-REMO2009 and CLMcom-ETH-COSMO-crCLIM-v1-1. Each GCM-RCM combination used is represented by a
 218 number (1, 3 or 12) indicating which realization of the GCM is used for the particular simulation.

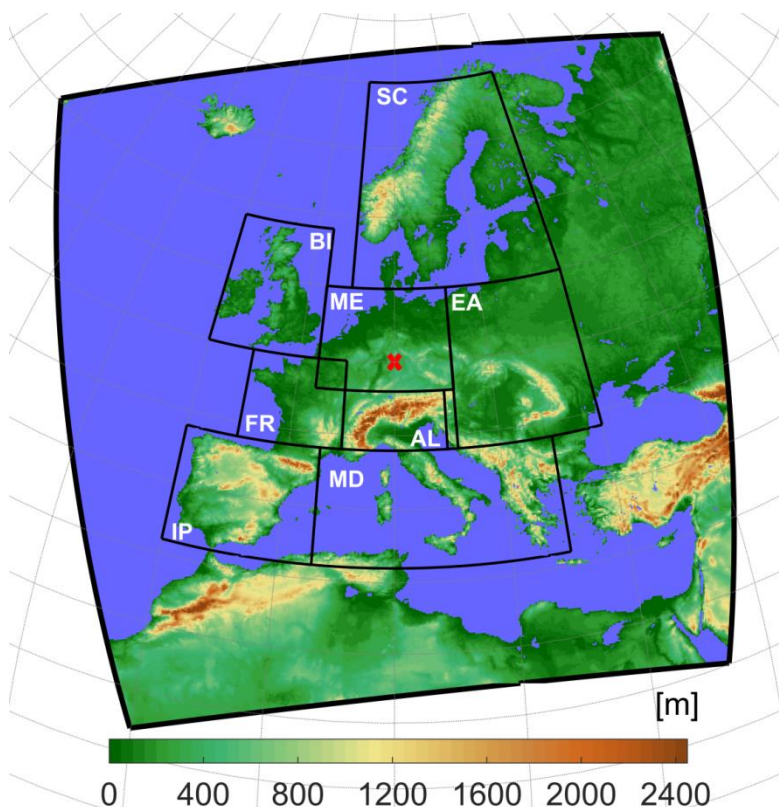
219

GCM \ RCM	RCA	CCLM	RACMO	HIRHAM	REMO	COSMO
ICHEC-EC-EARTH	r12		r1	r3		
MOHC-HadGEM2-ES	r1		r1	r1		
CNRM-CERFACS-CNRM-CM5	r1			r1		
MPI-M-MPI-ESM-LR	r1	r2		r1	r1	r1
IPSL-IPSL-CM5A-MR	r1					
NCC-NorESM1-M	r1			r1		r1
CCCma-CanESM2		r1				
MIROC-MIROC5		r1				

220

221

222



223

224 Figure 1. Map showing the EURO-CORDEX region (outer frame) with elevation in colours. PRUDENCE sub-regions (Christensen and
 225 Christensen, 2007) used in the analysis are also shown: BI = British Isles, IP = Iberian Peninsula, FR = France, ME = Mid-Europe, SC =
 226 Scandinavia, AL = Alps, MD = Mediterranean, EA = Eastern Europe. Red cross marks point used in Figure 4.

227

228 Generally, GCM results are quite comparable to reality, and many validation studies of GCMs exist, also
 229 with an eye on Europe (e.g. McSweeney et al., 2015). We are aware of the use in some papers of selection

230 procedures for selecting how to choose sub-sets of available GCMs (e.g. [McSweeney et al., 2015](#); [Rowell,](#)
231 [2019](#)). There is, however, no simple quality index that can be generally applied. Any discrimination of GCMs
232 depends on area, season, and the meteorological field and property being investigated ([Gleckler et al.,](#)
233 [2008](#); e.g. [their Fig. 9](#)). Furthermore, these tests and selection procedures are based on subjective
234 criteria and come with major caveats that impact the uncertainty range largely ([Madsen et al., 2017](#)). We
235 therefore choose, in accordance with most other similar studies, to use an ‘ensemble of opportunity’ for
236 the present study.
237

238 3 Methods

239 3.1 Duration

240 Extreme precipitation statistics are often described as a function of the time scale involved as intensity-
241 duration-frequency or depth-duration-frequency curves (e.g. [Overeem et al., 2008](#)). We consider two time
242 scales or *durations*. One is a duration of 1 h, which is simply the time series of hourly precipitation sums
243 available in each RCM grid point. The other is a duration of 24 h, where a 24 h sum is calculated in a sliding
244 window with a one hour time step. We will refer to these as hourly and daily duration, respectively. Our
245 daily duration corresponds to the traditional climatological practice of reporting daily sums but allows
246 heavy precipitation events to occur over two consecutive days. We also emphasize that the duration, as
247 defined here, is not the actual length of precipitation events in the model data, but is merely a concept to
248 define time scales.

249 3.2 Extreme value analysis

250 Extreme value analysis (EVA) provides methodologies to estimate high quantiles of a statistical distribution
251 from observations. The theory relies on fundamental convergence properties of time series of extreme
252 events; for details we refer to [Coles \(2001\)](#).
253

254 There are two main methodologies in EVA to obtain estimates of the high percentiles and the
255 corresponding return levels. In the *classical*, or *block maxima*, method, a generalised extreme value
256 distribution is fitted to the series of maxima over a time block, usually a year. Alternatively, in the *peak-*
257 *over-threshold* (POT) or *partial-duration-series* method, which is used here, all peaks with maximum above
258 a (high) threshold, x_0 , are considered. The peaks are assumed to occur independently at an average rate
259 per year of λ_0 . To ensure independence between peaks, a minimum time separation between peaks is
260 specified. Theory tells us, that when the threshold goes to infinity, the distribution of the exceedances
261 above the threshold, $x - x_0$, converges to a generalised Pareto distribution, whose cumulative distribution
262 function is

$$\mathcal{G}(x - x_0) = 1 - \left(1 + \xi \frac{x - x_0}{\sigma}\right)^{-\frac{1}{\xi}}, x > x_0$$

263 The parameter σ is the scale and is a measure of the width of the distribution. The parameter ξ is the shape
264 and describes the character of the upper tail of the GPD-distribution; $\xi > 0$ implies a heavy tail which
265 usually is the case for extreme precipitation events, while $\xi < 0$ implies a thin tail. Note that, quite
266 confusingly, an alternative sign convention of ξ occurs in the literature (e.g. [Hosking and Wallis, 1987](#)).
267

268 If we now consider an arbitrary level x with $x > x_0$, the average number of exceedances per year of x will
269 be

$$270 \lambda_x = \lambda_0 [1 - \mathcal{G}(x - x_0)]. \quad (1)$$

272
273 The T -year return level, x_T , is defined as the precipitation intensity which is exceeded on average once
274 every T years

$$\lambda_{x_T} T = 1$$

275 and by combining with (1) we get an expression for the return level x_T

$$276 \lambda_0 [1 - \mathcal{G}(x_T - x_0)] T = 1,$$

277
278 from which

$$279 x_T = \mathcal{G}^{-1} \left(1 - \frac{1}{\lambda_0 T} \right) + x_0. \quad (2)$$

280

281

282 Data points to be included in the POT analysis can be selected in two different ways. Either the threshold x_0
283 is specified and λ_0 is then a parameter to be determined or, alternatively, λ_0 is specified and x_0 determined
284 as a parameter. We choose the latter approach, since it is most convenient when working with data from
285 many different model simulations.

286

287 Choosing λ_0 is a point to consider: a too high value would include too few data points in the estimation and
288 a too low value implies the risk that the exceedances $x_T - x_0$ cannot be considered as GPD-distributed. We
289 choose $\lambda_0 = 3$ in accordance with Berg et al. (2019), which gives 75 data points for estimation for the 25
290 years long period time slices. Hosking and Wallis (1987) investigated the estimation of parameters of the
291 GPD-distribution and based on this warn against using the often applied maximum likelihood estimation for
292 a sample size below 500. Instead, they recommend probability-weighted moments and we have followed
293 this advice here.

294

295 We required a minimum of 3 and 24 h separation between peaks for 1 and 24 h duration, respectively. This
296 is in accordance with Berg et al. (2019) and furthermore, synoptic experience tells us that this will ensure
297 that neighbouring peaks are from independent weather systems. We found only a weak influence of these
298 choices on the results of our analysis.

299

300 In practical applications of EVA the parameters are estimated with large uncertainties due to limited length
301 of the time series. The threshold has the smallest relative uncertainty, the scale has a larger relative
302 uncertainty, and the shape has the largest relative uncertainty. Therefore, also the relative uncertainty of
303 the return levels increase with increasing T , as can be seen from Eq. 2.

304

305 **3.3 Bias adjustments and extreme value analysis**

306 The delta-change and bias correction approaches were introduced in general terms in Section 1. Now we
307 will formulate EVA-based analytical quantile-mapping based versions of the two approaches. In what
308 follows O_T is the T -year return levels estimated from present-day pseudo-observations ~~during the present~~

309 | ~~day period~~, while C_T (control) and S_T (scenario) denote the corresponding return levels, estimated from
 310 | present-day and end-21st-century model data, respectively. Finally, P_T (projection) denotes the end-21st-
 311 | century return level after bias-adjustment has been applied.
 312

313 | 3.3.1 Climate factor on the return levels (FAC)

314 | The simplest adjustment approach is to assume a climate factor on the return level (FAC)

$$P_T = \underbrace{S_T/C_T}_{\substack{\text{Delta-change} \\ \text{climate factor}}} \cdot O_T = \underbrace{O_T/C_T}_{\substack{\text{Bias correction} \\ \text{climate factor}}} \cdot S_T$$

315
 316 | We note that the delta-change and bias correction approach are identical for the FAC method.

317 | 3.3.2 Analytical quantile -mapping based on EVA

318
 319 | In the EVA-based quantile -mapping, two POT-based extreme value distributions with different parameters
 320 | are matched. Being more specific, we want to construct a transformation $x \rightarrow y$ defined by requiring that
 321 | exceedance rates above x and y , respectively, are equal for any x :

$$322 \quad \lambda_x = \lambda_y.$$

323 | This implies, according to (1), that

$$325 \quad \lambda_{0x}[1 - \mathcal{G}_x(x - x_0)] = \lambda_{0y}[1 - \mathcal{G}_y(y - y_0)],$$

326 | where \mathcal{G}_x is the GPD distribution of the exceedances $x - x_0$ and λ_{0x} the associated exceedance rate, and
 327 | \mathcal{G}_y and λ_{0y} are the similar entities for y .

329 | To simplify, we let $\lambda_{0x} = \lambda_{0y}$ (see Section 3.2) and therefore get

$$330 \quad \mathcal{G}_x(x - x_0) = \mathcal{G}_y(y - y_0),$$

331 | from which we obtain the transformation

$$332 \quad y = y_0 + \mathcal{G}_y^{-1}(\mathcal{G}_x(x - x_0)). \quad (3)$$

334 | For the delta-change approach (DC), the modelled GPD distribution functions for present-day and end-21st-
 335 | century conditions are quantile -mapped and the transformation obtained this way is then applied to
 336 | return levels determined from present-day pseudo-observations O_T . Thus the corresponding projected T -
 337 | year return level is according to Eq. (3)

$$338 \quad P_T = S_0 + \mathcal{G}_S^{-1}(\mathcal{G}_C(O_T - C_0)),$$

339 | where \mathcal{G}_C and \mathcal{G}_S are the GPD cumulative distribution functions for the modelled present-day (control) and
 340 | end-21st-century (scenario) data, respectively, and C_0 and S_0 are the corresponding threshold values.

341 | For the bias correction approach (BC), the present-day (control) and pseudo-observed GPD cumulative
 342 | distribution functions are quantile -mapped to obtain the model bias, which is then applied, using eq. (3), to
 343 | modelled end-21st-century (scenario) return levels.

$$345 \quad P_T = O_0 + \mathcal{G}_O^{-1}(\mathcal{G}_C(S_T - C_0)),$$

346 where G_O is the GPD cumulative distribution function for the observations and O_0 the corresponding
 347 threshold.

348 3.3.3 Reference adjustment methods

349 The performance of the bias adjustment methods described above will be compared with the performance
 350 of two reference adjustment methods, which are defined below. This is a similar to what is practice when
 351 verifying predictions, where the performance of the prediction should be superior to the performance of
 352 reference predictions, such as persistence or climatology.

353
 354 We choose two reference methods. One reference is to simply use, for a given model, the return level
 355 calculated from (pseudo-)observations as the projected return level (OBS),

$$P_T = O_T$$

356
 357 Another reference is to use the raw scenario model output data without any adjustment (SCE):

$$P_T = S_T.$$

358
 359
 360 For an overview of methods, see [Table 2](#)

361
 362 Table 2. Overview of methods used in the inter-comparison

OBS	(Pseudo-)observations (Reference method)
SCE	Raw RCM scenario (Reference method)
FAC	Climate factors -factor on return levels
DC	Quantile_-mapped delta-change based on EVA
BC	Quantile_-mapped bias correction based on EVA

363 3.4 The inter-model cross-validation procedure in detail

364
 365
 366 The inter-model cross-validation goes in detail as follows: Each of the N models are successively regarded
 367 as being pseudo-observations. The individual adjustment methods are calibrated on the present-day parts
 368 of the pseudo-observations and model return levels (present-day and end-21st-century), as appropriate
 369 depending on whether it is a bias correction or delta-change method. The calibration is done as described
 370 above. The adjustment methods are then applied to present-day observation and model data, again as
 371 appropriate, to obtain end-21st-century adjusted return levels. These are then validated against the end-
 372 21st-century return level from pseudo-observations.
 373

374
 375 The basic validation metric will be the relative error of end-21st-century return levels for a given duration
 376 and return period T :

$$RE = |P_T - V_T|/V_T$$

377
 378 i.e. the absolute difference between the projected return level P_T obtained from using adjustment and the
 381 validation return level V_T estimated from end-21st-century pseudo-observations, divided by the validation
 382 return level. This metric is calculated for every grid point and for every combination of model/pseudo-

383 observations. Since we have $N = 19$ model simulations in the ensemble, we have $N \times (N - 1) = 342$
 384 different combinations for validating each adjustment method and make statistics of the relative error. This
 385 quantifies the average performance of the different methods.

386
 387 User-end scenarios are often constructed as the median or mean from ensembles. We also tested this in
 388 the inter-model cross-validation setup. The calibration is performed as before on each of the remaining
 389 models and adjusted return levels for the end-21st-century calculated. But then the median of these
 390 adjusted future return levels is calculated and this is validated against the future pseudo-observations.
 391 Note that this gives only $N = 19$ different combinations and therefore a less robust statistics compared to
 392 above.

393

394 4 Results

395

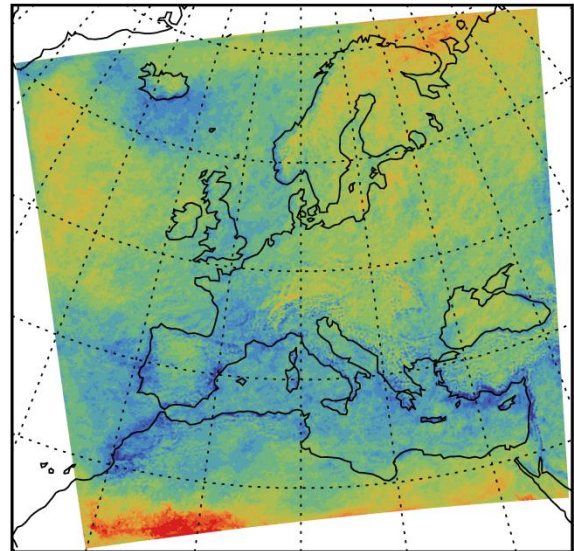
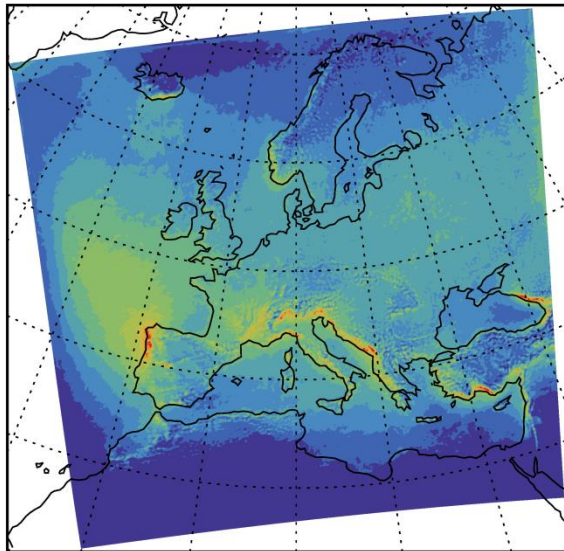
396 4.1 Modelled return levels for present-day and end-21st-century conditions

397

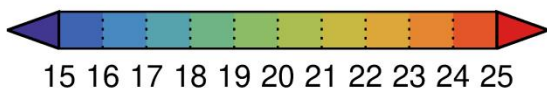
Return level, Duration: 1 h, Return period: 10 y

Present-day

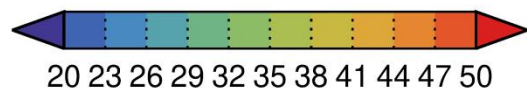
Rel. change
 Present-day to End-21st-century



mm



%



398

399 Figure 2. Geographical distribution of the 10 year-return level of precipitation intensity for 1 hour duration for present-day (left)
 400 and relative change from present-day to end-21st-century (right). In each grid point, values are the median return level over all 19
 401 model simulations.

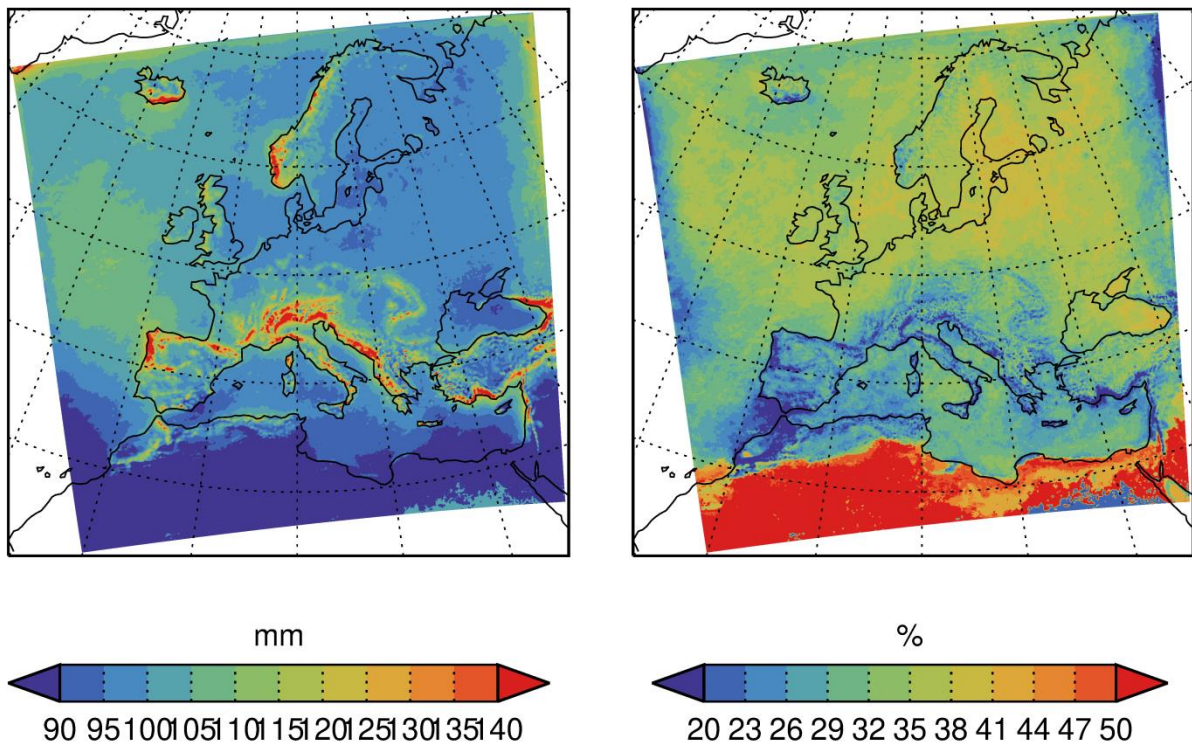
402

425 | [Figure 2](#) displays the geographical distribution of the 10-year return level for precipitation intensity of 1 h
 426 | duration, calculated as the median return level over all 19 model simulations. The smallest return levels are
 427 | mainly found in the arid North African region and to some extent in the Norwegian Sea, while the largest
 428 | return levels are found in southern Europe and in the Atlantic northwest of the Iberian Peninsula.
 429 | Mountainous regions, such as the Alps and western Norway stand out as have higher return levels than
 430 | their surroundings. This supports that the models are not totally unrealistic in modelling extreme
 431 | precipitation.

432 |
 433 | There is a general increase in the range of 20-40% from present-day to end-21st-century climatic
 434 | conditions. The relative changes are geographically quite uniform across the area. For instance, no evident
 435 | difference between land and sea appears. Likewise do the mountainous regions not stand out from the
 436 | surroundings.

437 |
 438 |

Return level, Duration: 24 h, Return period: 10 y
 Present-day Rel. change Present-day to End-21st-century

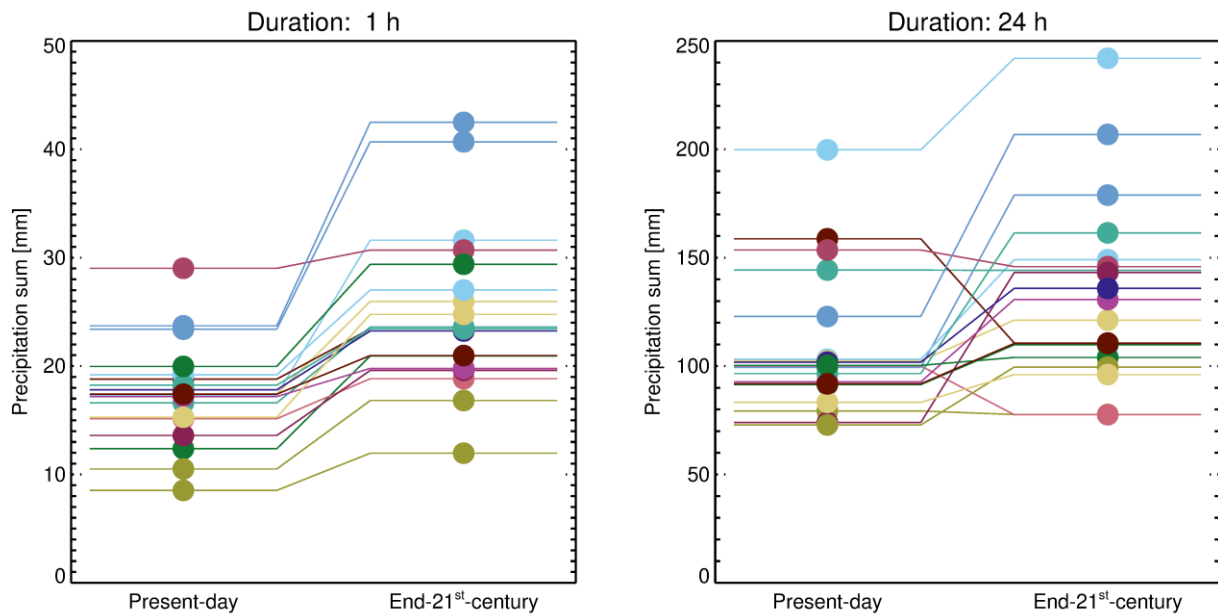


439 |
 440 | Figure 3. As [Figure 2](#) but for 24 h duration
 441 |

442 | We also show in [Figure 3](#) the median 10-year return level for 24 h duration. Again, the largest return levels
 443 | are found in southern Europe and northwest of the Iberian Peninsula. Also, the mountainous regions stand
 444 | out with higher return levels even more pronounced than for 1 h duration. The return levels generally
 445 | increase from present-day to end-21st-century conditions with around the same percentage as for 1 h
 446 | duration and also geographically homogeneous.

Form

447
448
449



450
451
452
453

Figure 4. Modelled return levels at 50N/10E (northern Germany, marked with 'X' in [Figure 1](#)) for present and future for 10 y return period and 1 h and 24 h durations. Different colours represent the 19 different GCM-RCM simulations listed in [Table 1](#).

454 To get a more detailed impression of the data, [Figure 4](#) shows return levels and their changes from present-day to end-21st-century for a grid point in Northern Germany for all 19 model simulations. For 1 h duration (left panel) return values increase from present-day to end-21st-century in all cases. For 24 h duration (right panel) typically the return levels increase from present-day to end-21st-century but with some exceptions. [This behaviour is common to all regions](#). For both durations, we also note the large spread in return levels within the ensemble. The spread is much higher than the change between present and future for most models; in other words: a poor signal to noise ratio. [This is probably a combined effect of different climate signals in different models and natural variability \(Aalbers et al., 2018\)](#).

462 4.2 Inter-model cross-validation

463

464 In the following, we will present results using two different types of display. First, we will use spatial maps of the median relative error, calculated from all combinations of model/pseudo-observations. Second, we will, for each adjustment method and for each combination of model/pseudo-observations, calculate the median relative error over each of the eight PRUDENCE sub-regions defined in Christensen and Christensen (2007) and shown on [Figure 1](#). For each region we will illustrate the distribution of the relative error across all combinations of model/pseudo-observations by showing the median and the 5/95-percentiles of this distribution.

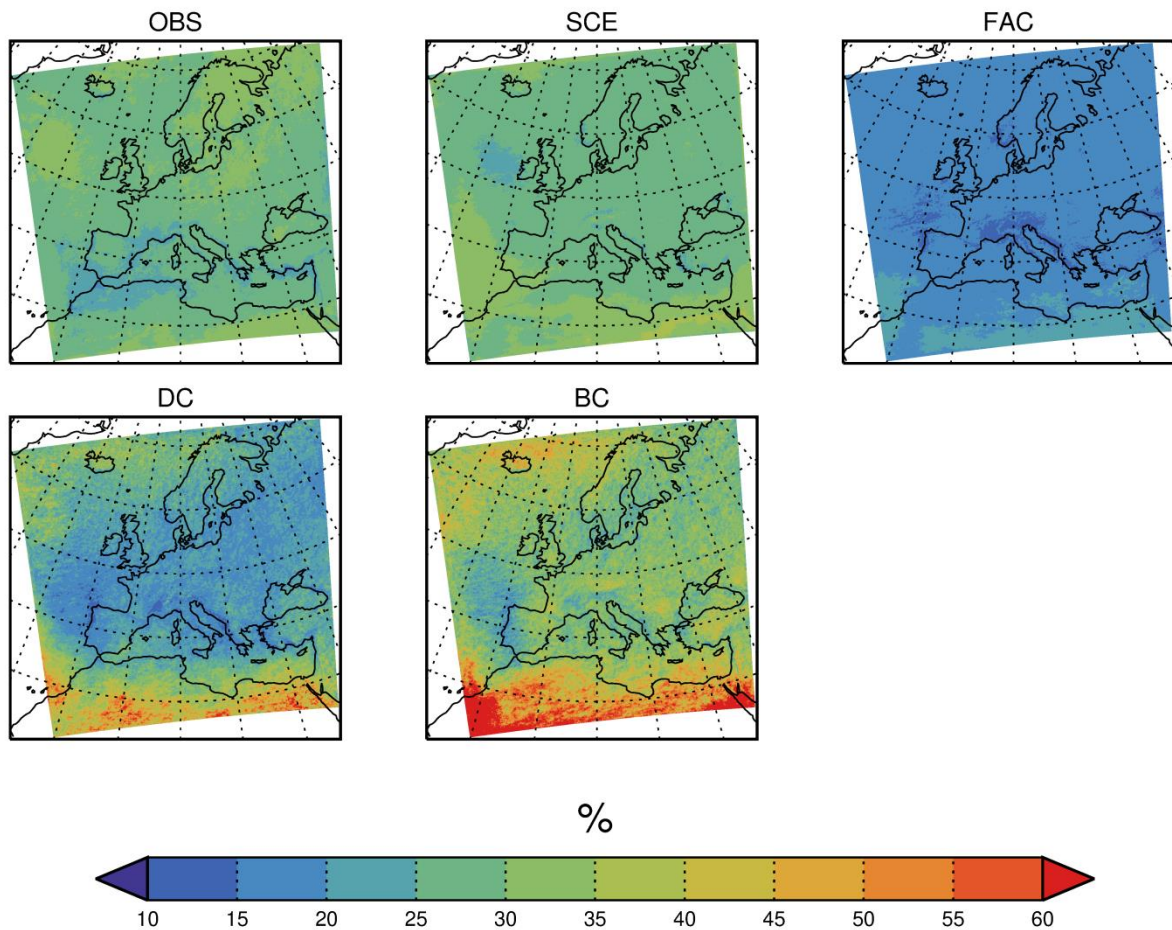
470

472 4.2.1 Results for 1 h duration

473

474 | **Figure 5** shows the median, across all model/pseudo-observations combinations, the relative error for all
 475 five methods for 1 h duration and 10 y return period.
 476

Relative error, Duration: 1 h, Return period: 10 y



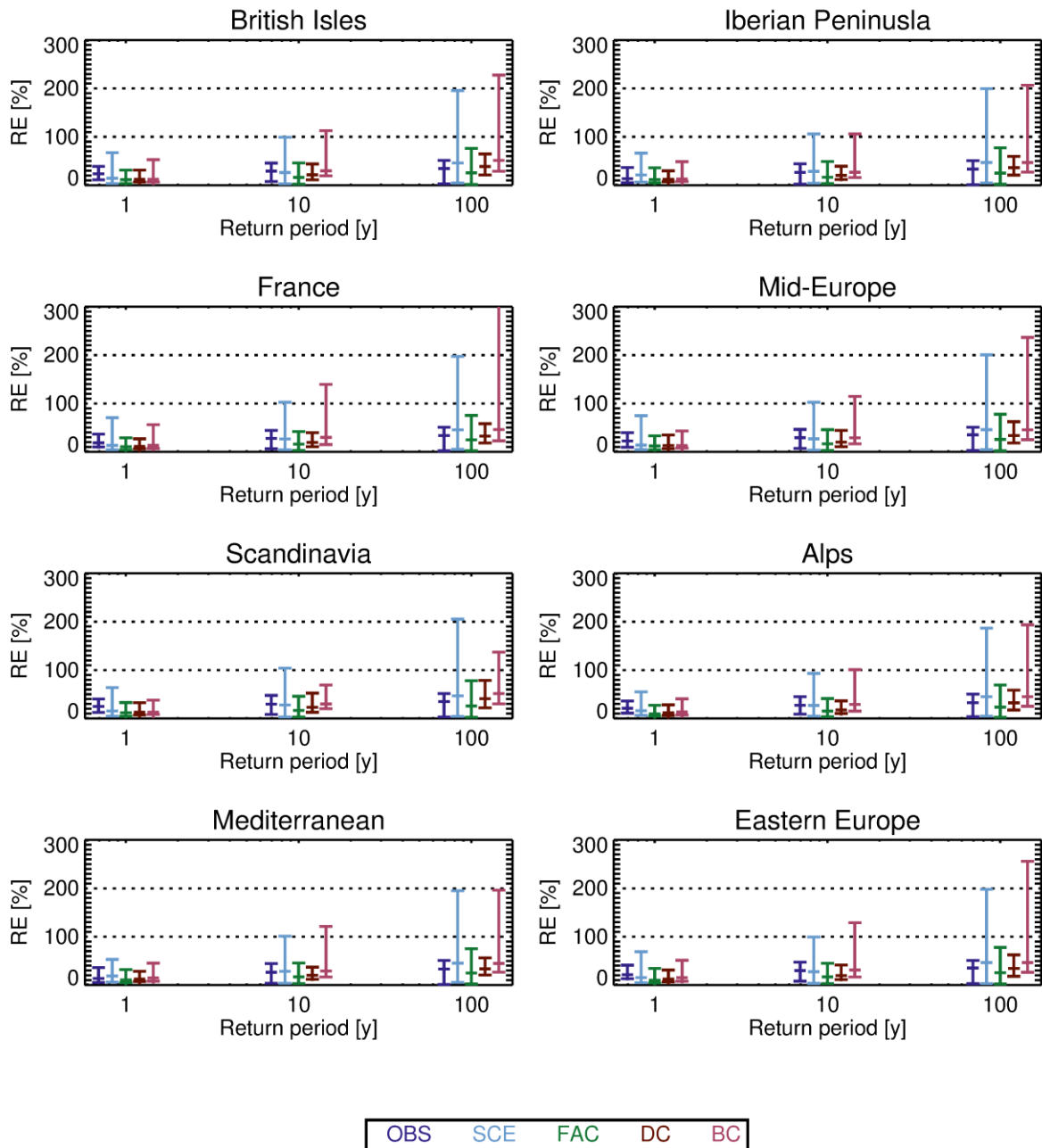
477
 478
 479 Figure 5. Geographical distribution of the relative error of end-21st-century 10 year return level for 1 h duration precipitation
 480 intensity from the inter-model cross-validation. Colours show the median of the relative error calculated over all model/pseudo-
 481 observations combinations. Panels are for the different adjustment methods.
 482

483 First we look at the reference methods. Relative errors from the OBS method are in the range of 20-40%.
 484 Lowest values are found in the Mediterranean, western France and the Atlantic west of the Mediterranean;
 485 highest values in the Atlantic west of Ireland and in Scandinavia. The SCE method has errors in the interval
 486 25-45%, lowest values in the Atlantic west of Ireland; largest values over parts of the Atlantic and northern
 487 Africa. The two reference methods give ~~on the whole~~ rather similar results, but the OBS method slightly
 488 outperforms SCE in the south, while the opposite is true in the north.
 489

490 The relative error of FAC is below 20% in most places. It is everywhere smaller than the relative error of the
 491 reference methods OBS and SCE. The DC method has a relative error comparable to (e.g. Western France,
 492 Western Iberia and Eastern Atlantic) or larger than (in particular in Northern Africa) that of FAC. That said,

493 the concept of relative error should be used with care in an arid region, such as Northern Africa. But from
 494 this result, it is not justified to use the more complicated DC, in favour of the simpler FAC. Finally, the
 495 relative error of BC is everywhere above both DC and FAC, indicating the poorest performance of all
 496 methods considered.
 497

Relative error, Duration: 1 h



498

499 Figure 6. Statistical distribution (median and 5th/95th percentile) of the relative error of the inter-model cross-validation for 1 hour
500 duration for 1 y, 10 y and 100 y return periods. Panels represent PRUDENCE sub-regions shown in [Figure 1](#). Each colour represents
501 a adjustment method (see [Table 2](#)).
502

503 The statistical distribution of the relative error is shown in [Figure 6](#) for the eight PRUDENCE sub-regions
504 (see [Figure 1](#)). We first note that the distribution of relative error is shifted towards higher values for larger
505 return periods, as expected. Next, we note that the two reference methods, OBS and SCE, behave
506 differently. SCE generally has a little larger median relative error, but the 95th percentile is much larger for
507 SCE than for OBS, in particular for large return periods. Thus, OBS overall performs better than SCE,
508 meaning that using present-day pseudo-observations to estimate projected end-21st-century return levels
509 yields better relative error than using raw modelled scenario data.
510

511 The FAC method generally has the best overall performance, both in terms of median and 95th percentile of
512 the relative error. The DC method has a slightly poorer performance than FAC, both in terms of the median
513 and the 95th percentile of the relative error. Finally, BC has poorer performance than DC, when comparing
514 the median of the relative error and in particular for the 95th percentile.
515

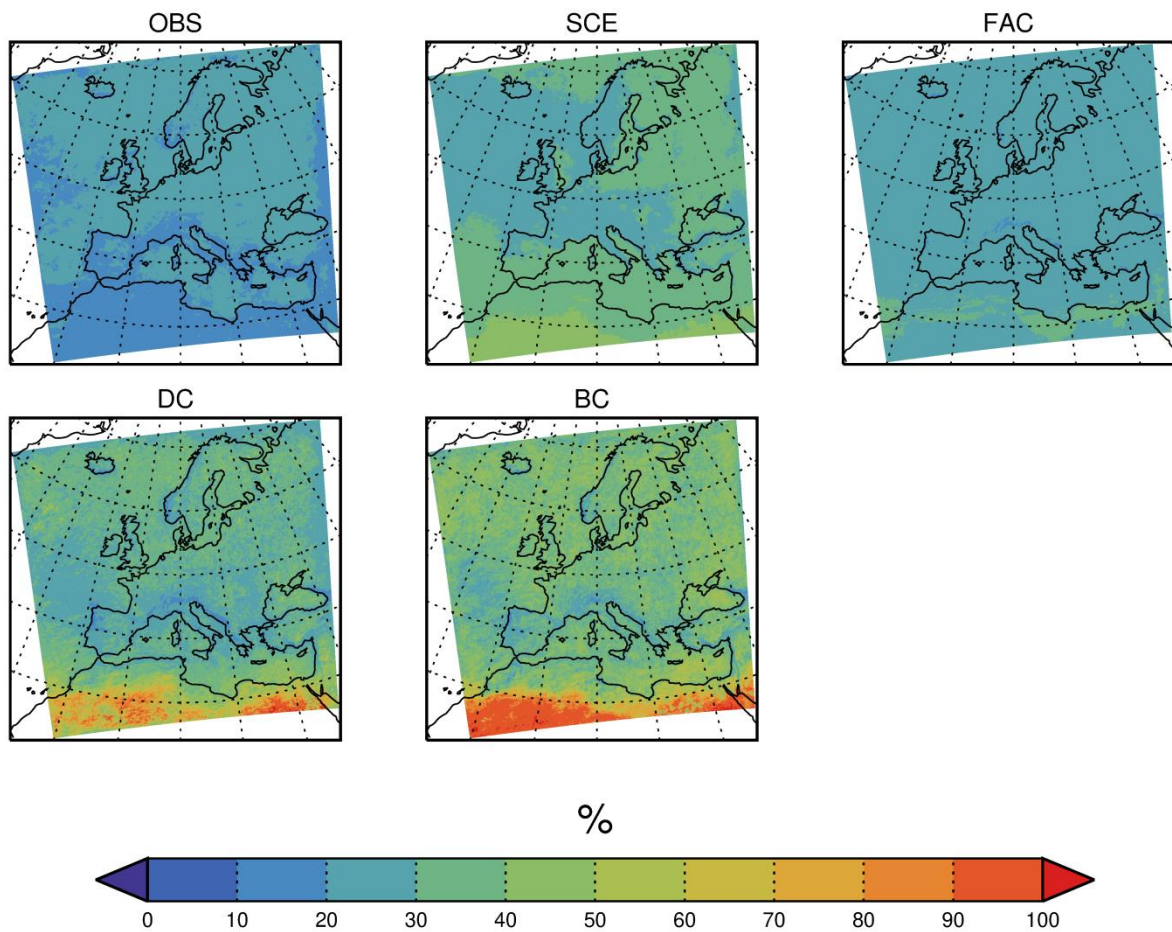
516 In summary, for 1 h duration, the method with the best performance is using a climate factor on the return
517 levels (FAC). This method outperforms both reference methods and the more sophisticated methods based
518 on quantile_-mapping, DC and BC, the latter having the poorest overall performance of them all. Note that
519 DC is comparing GPDs from the same model, whereas BC is comparing GPDs from different models. If the
520 difference, in terms of GPD parameters, between two models in the present-day climate is typically larger
521 than the difference between the same model in present-day and end-21st-century climate, it can explain
522 the different results.
523

524

525 4.2.2 Results for 24 h duration

526

Relative error, Duration: 24 h, Return period: 10 y



527

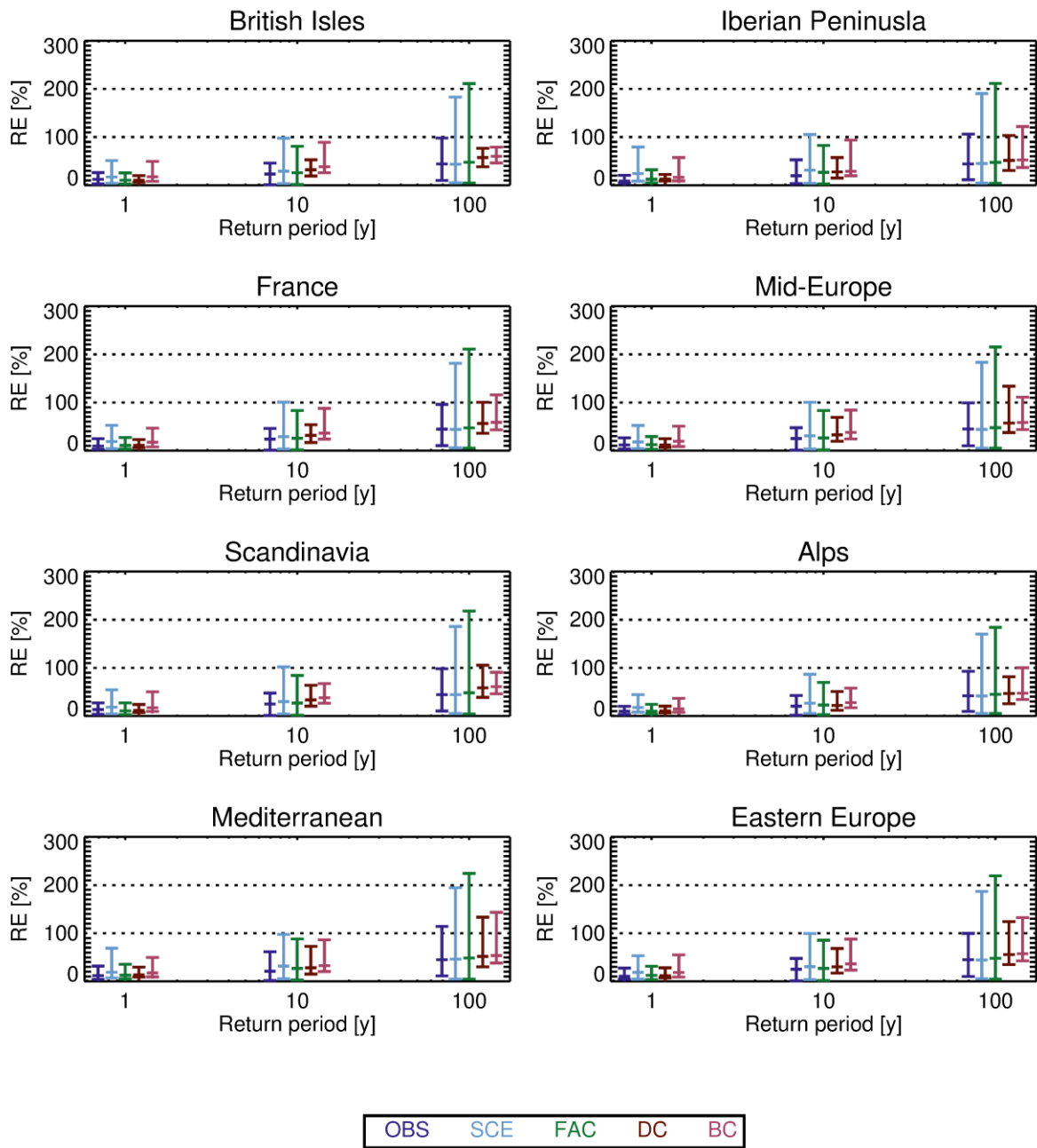
528 | Figure 7. As [Figure 5](#) but for 24 h duration.

529

530 | For 24 h duration (see [Figure 7](#)), OBS has the lowest median relative error (less than 30%) in most regions
531 | of all the adjustment methods, while SCE has higher relative error in the interval 30-60% approximately,
532 | with the highest values in North Africa. FAC has relative errors in-between those of OBS and SCE. Of the
533 | quantile_-mapping methods, DC has relative errors in the interval 20-80% approximately, larger than FAC in
534 | most places, and finally BC has, as for 1 h duration, the largest median relative errors of all the methods.

535

Relative error, Duration: 24 h



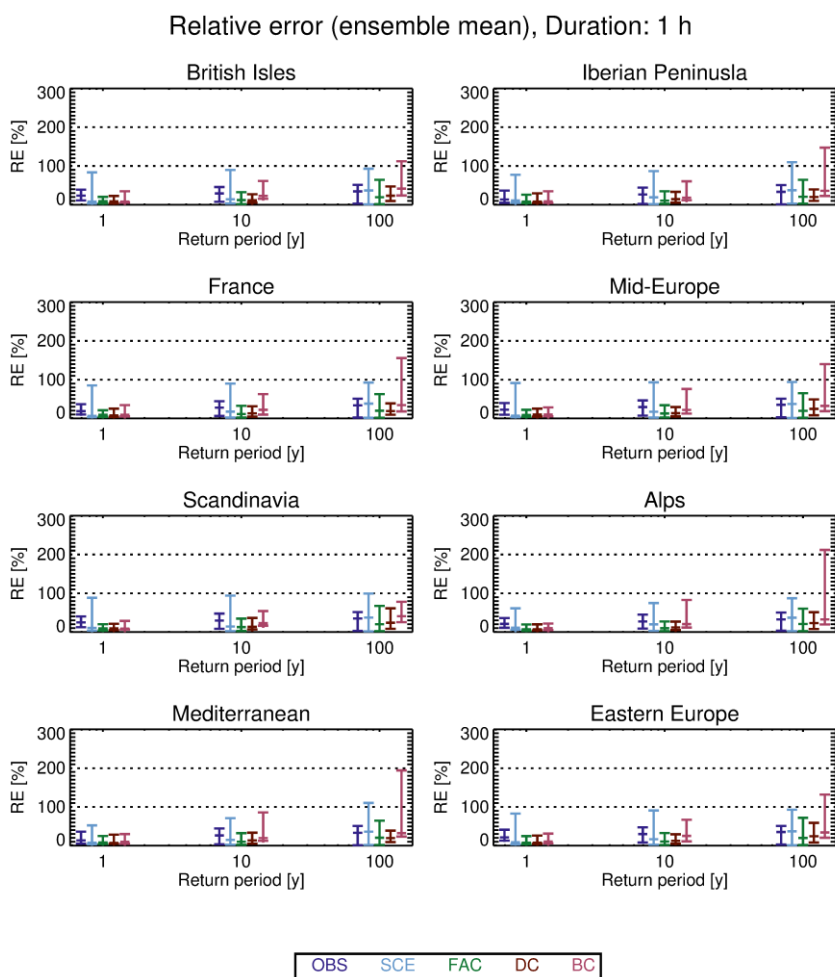
536
 537 | Figure 8. As [Figure 6](#) but for 24 h duration
 538

539 As for the 1 h duration, we also compare the entire statistical distribution of the relative error of the
 540 different adjustment methods for all three return periods ([Figure 8](#)), and again, both median and 95th
 541 percentile of the relative error increases for larger return periods, as expected. Further, OBS seems,
 542 surprisingly, to have a small median relative error and the smallest 95th percentile of all methods
 543 considered for all sub-regions. SCE has a median not too different from that of OBS, but the 95th percentile

544 | is much larger. Similar characteristics hold for FAC. The quantile_-mapping methods DC and BC have slightly
 545 | larger median values, but the 95th percentile is smaller than for FAC. All these characteristics hold for all
 546 | sub-regions.
 547

548 | 4.2.3 Ensemble median

549 | Also inter-model cross-validation of pseudo-observations against model ensemble median, as described in
 550 | Section 3.4, was carried out. For duration 1 h, distribution of the relative error is shown in Figure 9. By
 551 | comparing with [Figure 6](#), the distribution of the relative error does not change much overall. However, for
 552 | many of the sub-regions considered and for the longer return periods, the FAC and BC have a smaller 95th
 553 | percentile for cross-validation against model ensemble means, than against individual models.



554 |
 555 | Figure 9. As [Figure 6](#) but for inter-model cross-validation against ensemble medians.
 556

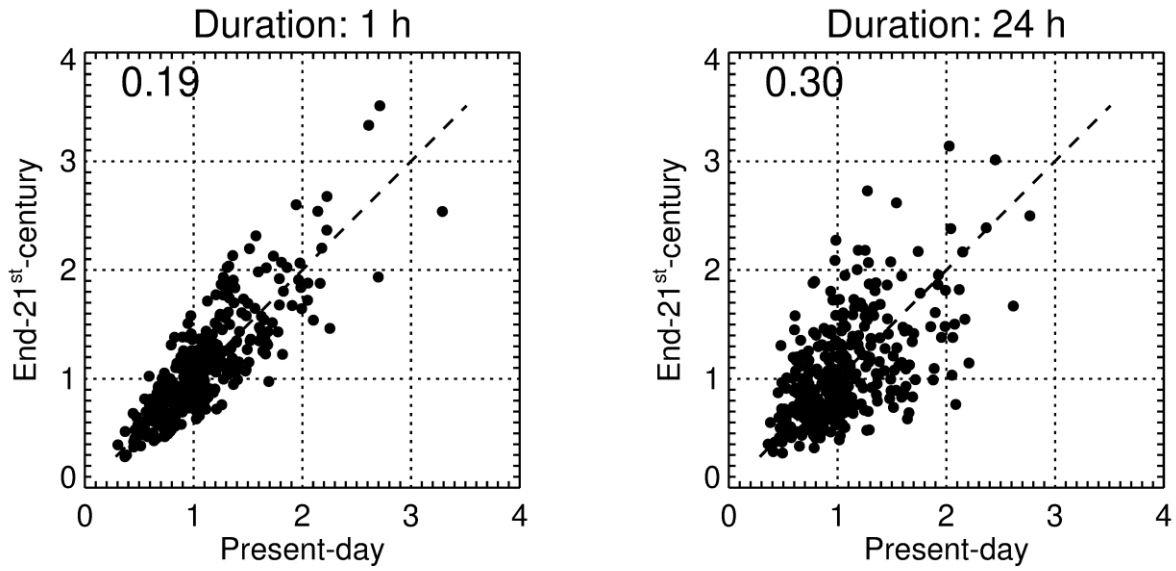
557 | Also for 24 h duration the distribution of the relative errors does not change much when shifting to
 558 | validation against ensemble median (not shown).

559 | 4.3 Further analysis on conditions for skill

560

561 To get further insight into the difference in performance between hourly and daily precipitation, we
 562 consider for a given return period the relationship between the bias factor for present-day $B_{P,T} = \frac{C_T}{O_T}$ and
 563 end-21st-century $B_{F,T} = \frac{S_T}{V_T}$ for all model/pseudo-observations combinations (see [Figure 10](#)).
 564

Bias factor of return level
 Region: Mid-Europe, Return period: 10 y



565
 566 Figure 10. Relationship between present-day and end-21st-century bias factors of 10-year return levels for Mid-Europe sub-region
 567 for all pseudo-observation/model combinations. Left panel: 1 h duration and right panel: 24 h duration. Numbers in upper left
 568 corners are the R indices. See text for details.
 569

570 In this figure, the relationship between present-day and end-21st-century bias factors appears more
 571 pronounced for 1 h duration than for 24 h duration. That said, it must be borne in mind that if the point
 572 (x, y) is in the plot, so is the point $(1/y, 1/x)$, and this implies an inherent tendency to a fan-like spread of
 573 points from $(0,0)$, as seen on both plots.
 574

575 To quantify the strength of the above relationship, we define an index:

576
$$R = \left\langle \frac{|B_F - B_P|}{(B_F + B_P)/2} \right\rangle,$$

577 where $\langle \cdot \rangle$ means averaging over combinations of model/pseudo-observations. This index is an extension of
 578 the index introduced by Maurer et al. ([2013](#)). It is the ensemble average of the relative absolute difference
 579 between the present-day and future bias. A value of $R = 0$ means these biases are equal, i.e. perfect
 580 stationarity; and the smaller the value of R , the closer to stationarity (in an ensemble sense).
 581

582 Values of R are given in the upper left corner of each panel of [Figure 10](#) and they also support the partial
 583 relationships described above, and a stronger one for hourly duration. These relations are important since
 584 they could explain the generally good performance of the FAC method seen in the previous section.

585 Suppose that $B_{P,T} = B_{F,T}$, then

586
$$P_T = \frac{S_T}{C_T} O_T = S_T \frac{O_T}{C_T} = S_T B_P = S_T B_F = S_T \frac{V_T}{S_T} = V_T$$

587

588 and the FAC method will therefore adjust perfectly.

589

590 We also note that daily data, due to the summation, would have less erratic behaviour than hourly and
591 therefore we would expect any relationship to be less masked by noise for daily data than for hourly data
592 from purely statistical grounds. Therefore, any explanation to why it is opposite should probably be found
593 in physics or details of modelling. We will discuss this further in Section 5.3.

594 **5 Discussion**

595

596 **5.1 Relation with other studies**

597

598 The study by Rätty et al. (2014) touches upon related issues to ours. However, our study includes smaller
599 temporal scales (hourly and daily) ~~than does their study~~ and higher return periods (up to 100 years vs. the
600 99.9th percentile of daily precipitation corresponding to a return period of around 3 years). Nevertheless,
601 the two studies agree in their main conclusion; namely that applying a bias adjustment seems to offer an
602 additional level of realism to the processed data series, including in the climate projections, as compared to
603 using unadjusted model results. The two studies both support, in agreement with our study, the somewhat
604 surprising conclusion that using present-day (pseudo-)observations as the scenario gives a skill comparable
605 to that of the bias adjustment methods.

606

607 Kallache et al. (2011) proposed a correction method for extremes, CDF-t, and obtained good validation
608 result with calibration/validation split of historical data from Southern France. The CDF-t method was
609 applied by Laflamme et al. (2016) on daily New England data and concludes that “downscaled results are
610 highly dependent on RCM and GCM model choice”.

611

612 **5.2 Convection in RCMs**

613 The grid spacing of present state-of-the-art RCMs available in large ensembles, such as CORDEX, is around
614 10 km, and at this resolution it is necessary to describe convection through parameterizations. This is
615 obviously an important deficit for our purpose, since this could represent a systematic bias in all our
616 simulations and therefore violate our underlying assumptions that the individual model simulations and the
617 real-world observations behave similarly in a physical sense. Thus, we do not promote naively applying the
618 presented adjustment methods to hourly data from these models. Instead, the present work should be
619 seen as a statistical exercise and the methods can in the future be applied to convection permitting model
620 simulations that better represent the convective process. The results from the present work would apply
621 equally to that case.

622

623 With the advent of convective-permitting models, a more realistic modelling of convective precipitation
624 events is within reach and a change in the characteristics of such events is seen (Kendon et al., 2017;
625 Lenderink et al., 2019; Prein et al., 2015). This next generation of convection-permitting RCMs with a grid
626 spacing of a few km allows a much better representation of the diurnal cycle and convective systems as a

627 | whole (Prein et al., 2015). With that in mind, we foresee redoing the analysis when a suitable ensemble of
628 | convective-permitting RCM simulations becomes available.

629

630 | **5.3 Stationarity of bias**

631 | The success of applying bias adjustment to climate model simulations is linked to the biases being
632 | stationary, i.e. present and future biases being more or less identical. In Section 4.3 we showed (in Figure
633 | 10) that this was the case for 1 h duration and less so for 24 h duration in our pseudo-reality setting. Such a
634 | relationship is an example of an emergent constraint (Collins et al., 2012). This is a model-based concept,
635 | originally introduced to explain that models which have a too warm (cold) present-day climate tend to have
636 | a relatively warmer (colder) future climate. The reason for this is that it is the same underlying physics
637 | which generates the present-day and future temperatures (Christensen and Boberg, 2012).

638

639 | We suggest that our observed emergent constraints could be explained in a similar manner; namely as a
640 | result of the Clausius-Clapeyron relation linking atmospheric temperature changes to changes in its
641 | humidity content and thereby precipitation changes. The change prescribed by the Clausius-Clapeyron
642 | equation is usually termed the thermodynamic contribution. In addition to this, there is a dynamic
643 | contribution and this may explain the differences between the hourly and daily relation seen in Figure 10.
644 | The rationale is that hourly extremes are entirely due to convective precipitation events with almost no
645 | dynamic contribution (Lenderink et al., 2019), while daily extremes are a mixture of convective events and
646 | large-scale strong precipitation, of which the latter has a more significant dynamic contribution (Pfahl et al.,
647 | 2017), causing the less marked emergent constraint for the daily time scale. This interpretation is also
648 | supported in Figure 4, in which daily precipitation sees some ‘crossovers’ (future return level
649 | smaller than present), whereas hourly precipitation does not have any crossovers.

650

651 | **5.4 The spatial scale**

652 | In the definition of model bias it is tacitly assumed that the observational dataset has the same spatial
653 | resolution as the model data. In practice, however, it is rarely possible to separate the bias from a spatial
654 | scale mismatch. For instance, if we compare modelled precipitation, which represents averages over a grid
655 | box, with rain gauge data, which represent a point, there can be a quite substantial mismatch for extreme
656 | events (Eggert et al., 2015; Haylock et al., 2008). Therefore, if the bias is adjusted towards such point
657 | values, it may lead to further complications (Maraun, 2013).

658

659 | Sometimes though, it is desirable to include the scale mismatch in the bias adjustment. Many impact
660 | models, e.g. hydrological models, are tuned to perform well with local observational data as input. This
661 | presents an additional challenge if this impact model is to be driven by climate model data for climate
662 | change studies, since the climate model will have biases in its climate characteristics (mean, variability, etc.)
663 | compared to those of the observed data. Applying the adjustment step, the hydrological model can rely on
664 | its calibration to observed conditions (Haerter et al., 2015; Refsgaard et al., 2014).

665

666 | **5.5 Adjustment methods not included in the study**

667 | Only the basic adjustment methods have been included in our study. The simple climate factor approach

668 | has been applied in numerous hydrological applications ([DeGaetano and Castellano, 2017](#); [Sunyer et al.,](#)
669 | [2015](#)) and others. We also wanted to test quantile_-mapping approaches, which in extreme value theory
670 | takes the form of a parametric transfer function. This we have applied in two flavours in the spirit of (Räty
671 | et al. [\(2014\)](#)). Finally, we wanted to benchmark against the ‘canonical’ benchmark methods: observations
672 | and raw model output.
673

674 | There is a myriad of more specialised methods, each tailored to account for a particular deficit of the
675 | simpler methods. First, there is the issue whether it for precipitation is more reasonable to map relative
676 | quantile changes rather than absolute ones ([Cannon et al., 2015](#)). It has also been argued that a bias
677 | correction method should preserve long-term trends, i.e. the ‘climate signal’ and only adjust the shorter
678 | time scales, as extensively discussed in ([Cannon et al., 2015](#)). Then multivariate methods have been argued
679 | for and applied in order to preserve relationships between variables ([Cannon, 2018](#)), and [nested methods](#)
680 | [to account for different biases for different time scales \(Mehrotra et al., 2018\)](#). Also methods to correct for
681 | systematic displacement of variable features in complex terrain have been suggested and applied ([Maraun](#)
682 | [and Widmann, 2015](#)). Finally, Li et al. [\(2018\)](#) adjusts stratiform and convective precipitation separately
683 | instead of adjusting the total precipitation. In this way, any future change in the ratio between the two
684 | types of precipitation is accounted for.
685

686 | It could be interesting to examine the above methods in future studies, though we acknowledge it would
687 | be a quite extensive work. We can at present only guess about the outcome of such work but the more
688 | refined methods may not perform too well in the inter-model cross-validation setting. The reason for this
689 | suspicion is that these methods, while being more elaborate, in most cases also have more parameters to
690 | be estimated, implying a higher risk of overfitting. An argument in favour of this is that the present study
691 | shows that the more elaborate quantile_-mapping methods DC og BC do not outperform the simpler FAC
692 | method.

693 | **6 Conclusions**

694 |
695 | Based on hourly precipitation data from a 19-member ensemble of climate simulations we have
696 | investigated the benefit of bias adjusting extreme precipitation return levels on hourly and daily time scales
697 | and evaluated the different methods. This is done in a pseudo-reality setting, where one model simulation
698 | in turn from the ensemble plays the role of observations extending into the future. The return levels
699 | obtained from each of the remaining model simulations are then adjusted in the present-day period, using
700 | different adjustment methods. Then the same adjustment methods are applied to end-21st-century model
701 | data to obtain projected return levels, which are then compared with the corresponding pseudo-realistic
702 | future return levels.
703

704 | The main result of this inter-comparison is that applying bias adjustment methods improves projected
705 | extreme precipitation return levels, compared to using the un-adjusted model runs. Can an overall superior
706 | adjustment methodology be appointed? For hourly duration, the method to recommend (having the
707 | smallest relative error) is the simple climate factor approach FAC, which is better in terms of the relative
708 | error than the more complicated analytical quantile_-mapping methods based on EVA, DC and, in particular,
709 | BC. For daily duration, the OBS method performs surprisingly well, having the smallest 95th percentile of

710 | the relative error. Furthermore, the quantile [mapping](#) methods perform better than FAC, with DC having
711 | the smallest relative error. These conclusions hold regardless of the sub-region considered. We also cross-
712 | validated against model ensemble means; this gave in general similar results without significant changes in
713 | the distribution of the relative error.

714

715 | Finally, we registered emergent constraints between present-day and end-21st-century biases. This was
716 | more pronounced for hourly than for daily time scales. This could be caused by hourly precipitation being
717 | more directly linked to the Clausius-Clapeyron response, but this requires more clarification in future work.

718

719

720 | *Data availability.* The hourly EURO-CORDEX precipitation data are not part of the standard suite of CORDEX
721 | and are therefore not produced nor shared by all modelling groups. The data used in this study may be
722 | obtained upon request from each modelling group. The IDL code used in the analysis can be obtained from
723 | TS.

724

725 | *Author contribution.* TS and PT designed the analysis with contribution from other co-authors and
726 | programmed the analysis software. PB, FB, OBC and PT prepared the data. TS prepared the manuscript with
727 | contributions from PT, PB, FB, OBC, BC, JHC, CS, and MSM.

728

729 | *Competing interests.* The authors declare that they have no conflict of interest.

730

731

732 | *Acknowledgements.* The work was supported by the European Commission through the Horizon 2020
733 | Programme for Research and Innovation under the EUCP project (Grant Agreement 776613). Part of the
734 | funding was provided by the Danish State through the Danish Climate Atlas. PB was funded by the project
735 | AQUACLEW, which is part of ERA4CS, an ERA-NET initiated by JPI Climate, and funded by FORMAS (SE), DLR
736 | (DE), BMWFW (AT), IFD (DK), MINECO (ES), ANR (FR) with co-funding by the European Commission (Grant
737 | Agreement 690462). Some of the simulations were performed in the COPERNICUS C3S project C3S_34b
738 | (PRINCIPLES). We acknowledge the World Climate Research Programme's Working Group on Regional
739 | Climate, and the Working Group on Coupled Modelling, former coordinating body of CORDEX and
740 | responsible panel for CMIP5. We thank the climate modelling groups (listed in [Table 1](#) of this paper)
741 | for producing and making their model output available. We also acknowledge the Earth System Grid
742 | Federation infrastructure, an international effort led by the U.S. Department of Energy's Program for
743 | Climate Model Diagnosis and Intercomparison, the European Network for Earth System Modelling and
744 | other partners in the Global Organisation for Earth System Science Portals (GO-ESSP). It is appreciated that
745 | Geert Lenderink, KNMI, Claas Teichmann, GERICS and Heimo Truhetz, University of Graz made model data
746 | of hourly precipitation available for analysis. [We appreciate constructive comments from referee Jorn van
747 | de Velde, from two anonymous referees, and from T. Kelder, R. L. Wilby, T. Marjoribanks, and L. Slater.](#)

748

749

750 | **References**

751

752 | [Aalbers, E. E., Lenderink, G., van Meijgaard, E. and van den Hurk, B. J. J. M.: Local-scale changes in mean
753 | and heavy precipitation in Western Europe, climate change or internal variability?, *Clim. Dyn.*, 50\(11–12\),
754 | 4745–4766, doi:10.1007/s00382-017-3901-9, 2018.](#)

755 [Arakawa, A.: The Cumulus Parameterization Problem: Past, Present, and Future, J. Clim., 17, 33, 2004.](#)

756 [Berg, P., Feldmann, H. and Panitz, H.-J.: Bias correction of high resolution regional climate model data, J.](#)
757 [Hydrol., 448–449, 80–92, doi:10.1016/j.jhydrol.2012.04.026, 2012.](#)

758 [Berg, P., Christensen, O. B., Klehmet, K., Lenderink, G., Olsson, J., Teichmann, C. and Yang, W.: Summertime](#)
759 [precipitation extremes in a EURO-CORDEX 0.11° ensemble at an hourly resolution, Nat. Hazards Earth Syst.](#)
760 [Sci., 19\(4\), 957–971, doi:10.5194/nhess-19-957-2019, 2019.](#)

761 [Boberg, F. and Christensen, J. H.: Overestimation of Mediterranean summer temperature projections due](#)
762 [to model deficiencies, Nat. Clim. Change, 2\(6\), 433–436, doi:10.1038/NCLIMATE1454, 2012.](#)

763 [Buser, C., Künsch, H. and Schär, C.: Bayesian multi-model projections of climate: generalization and](#)
764 [application to ENSEMBLES results, Clim. Res., 44\(2–3\), 227–241, doi:10.3354/cr00895, 2010.](#)

765 [Cannon, A. J.: Multivariate quantile mapping bias correction: an N-dimensional probability density function](#)
766 [transform for climate model simulations of multiple variables, Clim. Dyn., 50\(1–2\), 31–49,](#)
767 [doi:10.1007/s00382-017-3580-6, 2018.](#)

768 [Cannon, A. J., Sobie, S. R. and Murdock, T. Q.: Bias Correction of GCM Precipitation by Quantile Mapping:](#)
769 [How Well Do Methods Preserve Changes in Quantiles and Extremes?, J. Clim., 28\(17\), 6938–6959,](#)
770 [doi:10.1175/JCLI-D-14-00754.1, 2015.](#)

771 [Chen, J., Brissette, F. P. and Lucas-Picher, P.: Assessing the limits of bias-correcting climate model outputs](#)
772 [for climate change impact studies, J. Geophys. Res. Atmospheres, 120\(3\), 1123–1136,](#)
773 [doi:10.1002/2014JD022635, 2015.](#)

774 [Christensen, J. H. and Boberg, F.: Temperature dependent climate projection deficiencies in CMIP5 models,](#)
775 [Geophys. Res. Lett., 39, 24705, doi:10.1029/2012GL053650, 2012.](#)

776 [Christensen, J. H. and Christensen, O. B.: A summary of the PRUDENCE model projections of changes in](#)
777 [European climate by the end of this century, Clim. Change, 81\(S1\), 7–30, doi:10.1007/s10584-006-9210-7,](#)
778 [2007.](#)

779 [Coles, S.: An introduction to statistical modeling of extreme values, Springer., 2001.](#)

780 [Collins, M., Chandler, R. E., Cox, P. M., Huthnance, J. M., Rougier, J. and Stephenson, D. B.: Quantifying](#)
781 [future climate change, Nat. Clim. Change, 2\(6\), 403–409, doi:10.1038/nclimate1414, 2012.](#)

782 [DeGaetano, A. T. and Castellano, C. M.: Future projections of extreme precipitation intensity-duration-](#)
783 [frequency curves for climate adaptation planning in New York State, Clim. Serv., 5, 23–35,](#)
784 [doi:10.1016/j.cliser.2017.03.003, 2017.](#)

785 [Eggert, B., Berg, P., Haerter, J. O., Jacob, D. and Moseley, C.: Temporal and spatial scaling impacts on](#)
786 [extreme precipitation, Atmospheric Chem. Phys., 15\(10\), 5957–5971, doi:10.5194/acp-15-5957-2015, 2015.](#)

787 [Eyring, V., Bony, S., Meehl, G. A., Senior, C. A., Stevens, B., Stouffer, R. J. and Taylor, K. E.: Overview of the](#)
788 [Coupled Model Intercomparison Project Phase 6 \(CMIP6\) experimental design and organization, Geosci.](#)
789 [Model Dev., 9\(5\), 1937–1958, doi:10.5194/gmd-9-1937-2016, 2016.](#)

790 [Gleckler, P. J., Taylor, K. E. and Doutriaux, C.: Performance metrics for climate models, *J. Geophys. Res.*,](#)
791 [113\(D6\), D06104, doi:10.1029/2007JD008972, 2008.](#)

792 [Gudmundsson, L., Bremnes, J. B., Haugen, J. E. and Engen-Skaugen, T.: Technical Note: Downscaling RCM](#)
793 [precipitation to the station scale using statistical transformations – a comparison of methods, *Hydrol. Earth*](#)
794 [Syst. Sci., 16\(9\), 3383–3390, doi:10.5194/hess-16-3383-2012, 2012.](#)

795 [Gutiérrez, J. M., Maraun, D., Widmann, M., Huth, R., Hertig, E., Benestad, R., Roessler, O., Wibig, J., Wilcke,](#)
796 [R., Kotlarski, S., San Martín, D., Herrera, S., Bedia, J., Casanueva, A., Manzanar, R., Iturbide, M., Vrac, M.,](#)
797 [Dubrovsky, M., Ribalaygua, J., Pórtoles, J., Rätty, O., Räisänen, J., Hingray, B., Raynaud, D., Casado, M. J.,](#)
798 [Ramos, P., Zerenner, T., Turco, M., Bosshard, T., Štěpánek, P., Bartholy, J., Pongracz, R., Keller, D. E., Fischer,](#)
799 [A. M., Cardoso, R. M., Soares, P. M. M., Czernecki, B. and Pagé, C.: An intercomparison of a large ensemble](#)
800 [of statistical downscaling methods over Europe: Results from the VALUE perfect predictor cross-validation](#)
801 [experiment, *Int. J. Climatol.*, 39\(9\), 3750–3785, doi:10.1002/joc.5462, 2019.](#)

802 [Haerter, J. O., Hagemann, S., Moseley, C. and Piani, C.: Climate model bias correction and the role of](#)
803 [timescales, *Hydrol. Earth Syst. Sci.*, 15\(3\), 1065–1079, doi:10.5194/hess-15-1065-2011, 2011.](#)

804 [Haerter, J. O., Eggert, B., Moseley, C., Piani, C. and Berg, P.: Statistical precipitation bias correction of](#)
805 [gridded model data using point measurements, *Geophys. Res. Lett.*, 42\(6\), 1919–1929,](#)
806 [doi:10.1002/2015GL063188, 2015.](#)

807 [Hanel, M. and Buishand, T. A.: On the value of hourly precipitation extremes in regional climate model](#)
808 [simulations, *J. Hydrol.*, 393\(3–4\), 265–273, doi:10.1016/j.jhydrol.2010.08.024, 2010.](#)

809 [Haylock, M. R., Hofstra, N., Klein Tank, A. M. G., Klok, E. J., Jones, P. D. and New, M.: A European daily high-](#)
810 [resolution gridded data set of surface temperature and precipitation for 1950–2006, *J. Geophys. Res.*,](#)
811 [113\(D20\), doi:10.1029/2008JD010201, 2008.](#)

812 [Hosking, J. R. M. and Wallis, J. R.: Parameter and Quantile Estimation for the Generalized Pareto](#)
813 [Distribution, *Technometrics*, 29\(3\), 339, doi:10.2307/1269343, 1987.](#)

814 [Hui, Y., Chen, J., Xu, C., Xiong, L. and Chen, H.: Bias nonstationarity of global climate model outputs: The](#)
815 [role of internal climate variability and climate model sensitivity, *Int. J. Climatol.*, 39\(4\), 2278–2294,](#)
816 [doi:10.1002/joc.5950, 2019.](#)

817 [Jacob, D., Petersen, J., Eggert, B., Alias, A., Christensen, O. B., Bouwer, L. M., Braun, A., Colette, A., Déqué,](#)
818 [M., Georgievski, G., Georgopoulou, E., Gobiet, A., Menut, L., Nikulin, G., Haensler, A., Hempelmann, N.,](#)
819 [Jones, C., Keuler, K., Kovats, S., Kröner, N., Kotlarski, S., Kriegsmann, A., Martin, E., van Meijgaard, E.,](#)
820 [Moseley, C., Pfeifer, S., Preuschmann, S., Radermacher, C., Radtke, K., Rechid, D., Rounsevell, M.,](#)
821 [Samuelsson, P., Somot, S., Soussana, J.-F., Teichmann, C., Valentini, R., Vautard, R., Weber, B. and Yiou, P.:](#)
822 [EURO-CORDEX: new high-resolution climate change projections for European impact research, *Reg.*](#)
823 [Environ. Change, 14\(2\), 563–578, doi:10.1007/s10113-013-0499-2, 2014.](#)

824 [Kallache, M., Vrac, M., Naveau, P. and Michelangeli, P.-A.: Nonstationary probabilistic downscaling of](#)
825 [extreme precipitation, *J. Geophys. Res.*, 116\(D5\), doi:10.1029/2010JD014892, 2011.](#)

826 [Kendon, E. J., Roberts, N. M., Fowler, H. J., Roberts, M. J., Chan, S. C. and Senior, C. A.: Heavier summer](#)
827 [downpours with climate change revealed by weather forecast resolution model, *Nat. Clim. Change*, 4\(7\),](#)
828 [570–576, doi:10.1038/nclimate2258, 2014.](#)

829 [Kendon, E. J., Ban, N., Roberts, N. M., Fowler, H. J., Roberts, M. J., Chan, S. C., Evans, J. P., Fosser, G. and](#)
830 [Wilkinson, J. M.: Do Convection-Permitting Regional Climate Models Improve Projections of Future](#)
831 [Precipitation Change?, Bull. Am. Meteorol. Soc., 98\(1\), 79–93, doi:10.1175/BAMS-D-15-0004.1, 2017.](#)

832 [Kerkhoff, C., Künsch, H. R. and Schär, C.: Assessment of Bias Assumptions for Climate Models, J. Clim.,](#)
833 [27\(17\), 6799–6818, doi:10.1175/JCLI-D-13-00716.1, 2014.](#)

834 [Klemeš, V.: Operational testing of hydrological simulation models, Hydrol. Sci. J., 31\(1\), 13–24,](#)
835 [doi:10.1080/02626668609491024, 1986.](#)

836 [Laflamme, E. M., Linder, E. and Pan, Y.: Statistical downscaling of regional climate model output to achieve](#)
837 [projections of precipitation extremes, Weather Clim. Extrem., 12, 15–23, doi:10.1016/j.wace.2015.12.001,](#)
838 [2016.](#)

839 [Lenderink, G., Belušić, D., Fowler, H. J., Kjellström, E., Lind, P., van Meijgaard, E., van Ulft, B. and de Vries,](#)
840 [H.: Systematic increases in the thermodynamic response of hourly precipitation extremes in an idealized](#)
841 [warming experiment with a convection-permitting climate model, Environ. Res. Lett., 14\(7\), 074012,](#)
842 [doi:10.1088/1748-9326/ab214a, 2019.](#)

843 [Li, J., Evans, J., Johnson, F. and Sharma, A.: A comparison of methods for estimating climate change impact](#)
844 [on design rainfall using a high-resolution RCM, J. Hydrol., 547, 413–427, doi:10.1016/j.jhydrol.2017.02.019,](#)
845 [2017a.](#)

846 [Li, J., Johnson, F., Evans, J. and Sharma, A.: A comparison of methods to estimate future sub-daily design](#)
847 [rainfall, Adv. Water Resour., 110, 215–227, doi:10.1016/j.advwatres.2017.10.020, 2017b.](#)

848 [Li, J., Sharma, A., Evans, J. and Johnson, F.: Addressing the mischaracterization of extreme rainfall in](#)
849 [regional climate model simulations – A synoptic pattern based bias correction approach, J. Hydrol., 556,](#)
850 [901–912, doi:10.1016/j.jhydrol.2016.04.070, 2018.](#)

851 [Madsen, M. S., Langen, P. L., Boberg, F. and Christensen, J. H.: Inflated Uncertainty in Multimodel-Based](#)
852 [Regional Climate Projections, Geophys. Res. Lett., 44\(22\), 2017GL075627, doi:10.1002/2017GL075627,](#)
853 [2017.](#)

854 [Maraun, D.: Nonstationarities of regional climate model biases in European seasonal mean temperature](#)
855 [and precipitation sums, Geophys. Res. Lett., 39\(6\), n/a-n/a, doi:10.1029/2012GL051210, 2012.](#)

856 [Maraun, D.: Bias Correction, Quantile Mapping, and Downscaling: Revisiting the Inflation Issue, J. Clim.,](#)
857 [26\(6\), 2137–2143, doi:10.1175/JCLI-D-12-00821.1, 2013.](#)

858 [Maraun, D.: Bias Correcting Climate Change Simulations - a Critical Review, Curr. Clim. Change Rep., 2\(4\),](#)
859 [211–220, doi:10.1007/s40641-016-0050-x, 2016.](#)

860 [Maraun, D. and Widmann, M.: The representation of location by a regional climate model in complex](#)
861 [terrain, Hydrol. Earth Syst. Sci., 19\(8\), 3449–3456, doi:10.5194/hess-19-3449-2015, 2015.](#)

862 [Maraun, D., Shepherd, T. G., Widmann, M., Zappa, G., Walton, D., Gutiérrez, J. M., Hagemann, S., Richter, I.,](#)
863 [Soares, P. M. M., Hall, A. and Mearns, L. O.: Towards process-informed bias correction of climate change](#)
864 [simulations, Nat. Clim. Change, 7\(11\), 764–773, doi:10.1038/nclimate3418, 2017.](#)

865 [Maurer, E. P., Das, T. and Cayan, D. R.: Errors in climate model daily precipitation and temperature output:](#)
866 [time invariance and implications for bias correction, Hydrol. Earth Syst. Sci., 17\(6\), 2147–2159,](#)
867 [doi:10.5194/hess-17-2147-2013, 2013.](#)

868 [McSweeney, C. F., Jones, R. G., Lee, R. W. and Rowell, D. P.: Selecting CMIP5 GCMs for downscaling over](#)
869 [multiple regions, Clim. Dyn., 44\(11–12\), 3237–3260, doi:10.1007/s00382-014-2418-8, 2015.](#)

870 [Mehrotra, R., Johnson, F. and Sharma, A.: A software toolkit for correcting systematic biases in climate](#)
871 [model simulations, Environ. Model. Softw., 104, 130–152, doi:10.1016/j.envsoft.2018.02.010, 2018.](#)

872 [Olsson, J., Berg, P. and Kawamura, A.: Impact of RCM Spatial Resolution on the Reproduction of Local,](#)
873 [Subdaily Precipitation, J. Hydrometeorol., 16\(2\), 534–547, doi:10.1175/JHM-D-14-0007.1, 2015.](#)

874 [Overeem, A., Buishand, A. and Holleman, I.: Rainfall depth-duration-frequency curves and their](#)
875 [uncertainties, J. Hydrol., 348\(1–2\), 124–134, doi:10.1016/j.jhydrol.2007.09.044, 2008.](#)

876 [Pfahl, S., O’Gorman, P. A. and Fischer, E. M.: Understanding the regional pattern of projected future](#)
877 [changes in extreme precipitation, Nat. Clim. Change, 7\(6\), 423–427, doi:10.1038/nclimate3287, 2017.](#)

878 [Piani, C., Haerter, J. O. and Coppola, E.: Statistical bias correction for daily precipitation in regional climate](#)
879 [models over Europe, Theor. Appl. Climatol., 99\(1–2\), 187–192, doi:10.1007/s00704-009-0134-9, 2010.](#)

880 [Prein, A. F., Langhans, W., Fosser, G., Ferrone, A., Ban, N., Goergen, K., Keller, M., Tölle, M., Gutjahr, O.,](#)
881 [Feser, F., Brisson, E., Kollet, S., Schmidli, J., Lipzig, N. P. M. and Leung, R.: A review on regional convection-](#)
882 [permitting climate modeling: Demonstrations, prospects, and challenges, Rev. Geophys., 53\(2\), 323–361,](#)
883 [doi:10.1002/2014RG000475, 2015.](#)

884 [Räisänen, J. and Räty, O.: Projections of daily mean temperature variability in the future: cross-validation](#)
885 [tests with ENSEMBLES regional climate simulations, Clim. Dyn., 41\(5–6\), 1553–1568, doi:10.1007/s00382-](#)
886 [012-1515-9, 2013.](#)

887 [Räty, O., Räisänen, J. and Ylhäisi, J. S.: Evaluation of delta change and bias correction methods for future](#)
888 [daily precipitation: intermodel cross-validation using ENSEMBLES simulations, Clim. Dyn., 42\(9–10\), 2287–](#)
889 [2303, doi:10.1007/s00382-014-2130-8, 2014.](#)

890 [Refsgaard, J. C., Madsen, H., Andréassian, V., Arnbjerg-Nielsen, K., Davidson, T. A., Drews, M., Hamilton, D.](#)
891 [P., Jeppesen, E., Kjellström, E., Olesen, J. E., Sonnenborg, T. O., Trolle, D., Willems, P. and Christensen, J. H.:](#)
892 [A framework for testing the ability of models to project climate change and its impacts, Clim. Change,](#)
893 [122\(1–2\), 271–282, doi:10.1007/s10584-013-0990-2, 2014.](#)

894 [Rowell, D. P.: An Observational Constraint on CMIP5 Projections of the East African Long Rains and](#)
895 [Southern Indian Ocean Warming, Geophys. Res. Lett., 46\(11\), 6050–6058, doi:10.1029/2019GL082847,](#)
896 [2019.](#)

897 [Sunyer, M., Luchner, J., Onof, C., Madsen, H. and Arnbjerg-Nielsen, K.: Assessing the importance of spatio-](#)
898 [temporal RCM resolution when estimating sub-daily extreme precipitation under current and future](#)
899 [climate conditions, Int. J. Climatol., 37\(2\), 688–705, 2017.](#)

900 [Sunyer, M. A., Gregersen, I. B., Rosbjerg, D., Madsen, H., Luchner, J. and Arnbjerg-Nielsen, K.: Comparison](#)
901 [of different statistical downscaling methods to estimate changes in hourly extreme precipitation using RCM](#)
902 [projections from ENSEMBLES, Int. J. Climatol., 35\(9\), 2528–2539, doi:10.1002/joc.4138, 2015.](#)

903 [Taylor, K. E., Stouffer, R. J. and Meehl, G. A.: An Overview of CMIP5 and the Experiment Design, Bull. Am.](#)
904 [Meteorol. Soc., 93\(4\), 485–498, doi:10.1175/BAMS-D-11-00094.1, 2012.](#)

905 [Thiemeßl, M. J., Gobiet, A. and Leuprecht, A.: Empirical-statistical downscaling and error correction of daily](#)
906 [precipitation from regional climate models, Int. J. Climatol., 31\(10\), 1530–1544, doi:10.1002/joc.2168,](#)
907 [2011.](#)

908 [Thiemeßl, M. J., Gobiet, A. and Heinrich, G.: Empirical-statistical downscaling and error correction of](#)
909 [regional climate models and its impact on the climate change signal, Clim. Change, 112\(2\), 449–468,](#)
910 [doi:10.1007/s10584-011-0224-4, 2012.](#)

911 [Trenberth, K. E., Dai, A., Rasmussen, R. M. and Parsons, D. B.: The Changing Character of Precipitation, Bull.](#)
912 [Am. Meteorol. Soc., 84\(9\), 1205–1218, doi:10.1175/BAMS-84-9-1205, 2003.](#)

913 [Van Schaeybroeck, B. and Vannitsem, S.: Assessment of calibration assumptions under strong climate](#)
914 [changes, Geophys. Res. Lett., 43\(3\), 1314–1322, doi:10.1002/2016GL067721, 2016.](#)

915 [Velázquez, J. A., Troin, M., Caya, D. and Brissette, F.: Evaluating the Time-Invariance Hypothesis of Climate](#)
916 [Model Bias Correction: Implications for Hydrological Impact Studies, J. Hydrometeorol., 16\(5\), 2013–2026,](#)
917 [doi:10.1175/JHM-D-14-0159.1, 2015.](#)

918
919